Seismica

Supporting Information for

Using ruptures from an earthquake cycle simulator to test geodetic early warning system performance

M. M. Solares-Colón[1], D. Melgar[1], A. Howell[2], B. Crowell[3], E. D'Anastasio[2], E. Caballero[2], and B. Fry[2]

[1]Department of Earth Sciences, University of Oregon, Eugene, Oregon, U.S.A.
[2]Earth Sciences New Zealand Te Pū Ao, Lower Hutt, Aotearoa, New Zealand
[3]School of Earth Sciences, The Ohio State University, Columbus, Ohio, U.S.A.

Contents of this file

Introduction

This supplement contains auxiliary information on methods and results. **Table S1** (modified from Hughes et al., 2025) provides input parameters used in Rate and State Earthquake Simulator (RSQSim; Richards-Dinger & Dieterich, 2012) to generate rupture scenario catalog. **Table S2** (modified from Goldberg et al., 2021) provides the GNSS Ground Motion Model coefficients used for waveform validation and for testing the Geodetic First Approximation of Size and Timing (G-FAST; Crowell et al., 2016, Crowell et al., 2018) early earthquake warning algorithm in this study. **Figure S1** shows the spatial distribution and magnitude range of events from both catalogs, RSQSim and FakeQuakes, used in this study. **Figure S2** illustrates the discrepancies between hypocenters and centroids for each rupture scenario, comparing the original rupture locations with geodetic CMT estimates from G-FAST. **Figure S3** highlights an extraordinary case of a full-rupture event in the Kermadec-Tonga subduction system, where G-FAST was unable to produce a solution.

Model Parameter	$Trench_{Lock}$ Value
Rate and state (*a* value)	0.001
Rate and state (*b* value)	0.004
Coefficient of friction (μ_0)	0.6
Rate and state (D_c)	$1x10^{-5}$
Rate and state (α_0)	0.25
Rate and state (θ_0)	$2x10^{8}$
Initial shear stress (τ_0)	60
Initial normal stress (σ_0)	100
Slip-deficit Model (HSM)	Trench creep model used in the NSHM 2022
Slip-deficit Model (TKSZ)	20% of the plate rate between ~37˚S to ~29˚S, and 50% of the plate rate from ~29˚S to ~25˚S

Table S1. Summary of the input parameters in RSQSim used to generate rupture scenario catalog (for details refer to Hughes et al., 2025); Hikurangi Subduction Margin (HSM); New Zealand National Seismic Hazard Model 2022 (NSHM 2022); Tonga-Kermadec Subduction Zone (TKSZ).

Study	A	B	C
Crowell et al. (2016)*	-6.687	1.500	-0.214
Goldberg et al. (2021)**	-3.841	0.937	-0.127

** Crowell et al. (2016) PGD scaling uses hypocentral distance and applies exponential distance weighting to favor stations closer to the source.*
*** Goldberg et al. (2021) PGD scaling uses generalized mean rupture distance.*

Table S2. GNSS Ground Motion Model coefficients for waveform validation and G-FAST testing. For waveform validation we use Goldberg et al. (2021) using the generalized mean rupture distance, R_p, with a value of – 2.3 for the power of the mean (p). The advantage of using R_p as a distance metric is that it allows for a more realistic treatment of a finite source as opposed to assuming a large rupture is a point source (e.g. as with the hypocenter distance; for more details refer to Goldberg et al. 2021). G-FAST PGD scaling applies exponential weighting as a function of epicentral distance to prioritize stations closer to source, using a minimum of four stations and a 3 km/s travel-time mask to exclude those that have not yet experienced strong ground shaking, enabling rapid characterization of large events (for more details refer to Crowell et al., 2016).

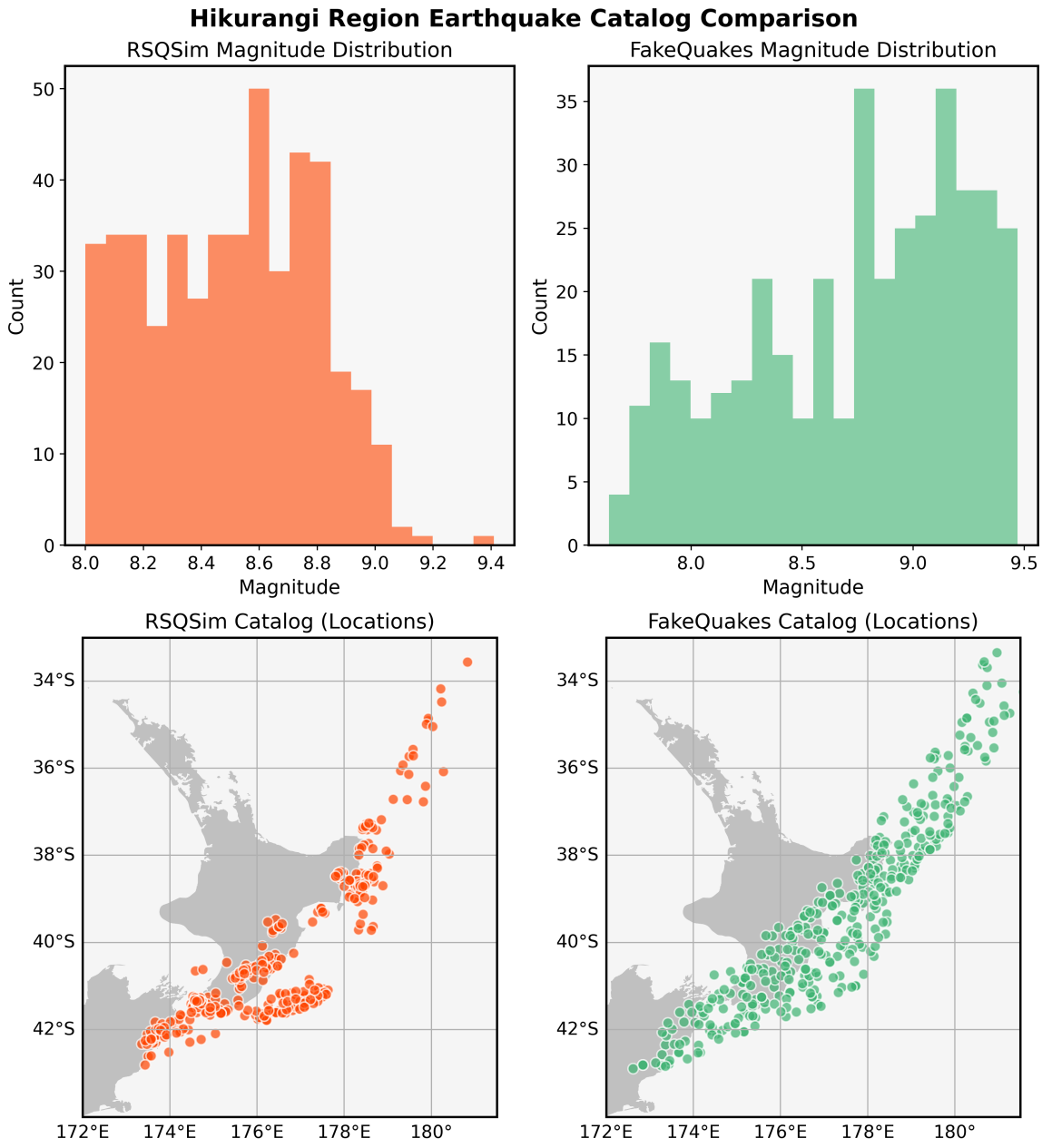

Figure S1. Comparison of the two synthetic earthquake catalogs for New Zealand: RSQSim (in orange) and FakeQuakes (in green). Top panels show the magnitude distribution of earthquakes (histograms) for each catalog, while bottom panels show the spatial distribution of earthquakes (epicenters represented by circles) over the Hikurangi region. Both catalogs exhibit a similar geographic extent but show differences in event density and magnitude distributions that reflect variations in catalog generation methods. RSQSim represents a long-term synthetic seismicity history based on physics-based modeling, whereas FakeQuakes provides a more comprehensive suite of rupture scenarios designed to explore a wide range of magnitudes and locations.

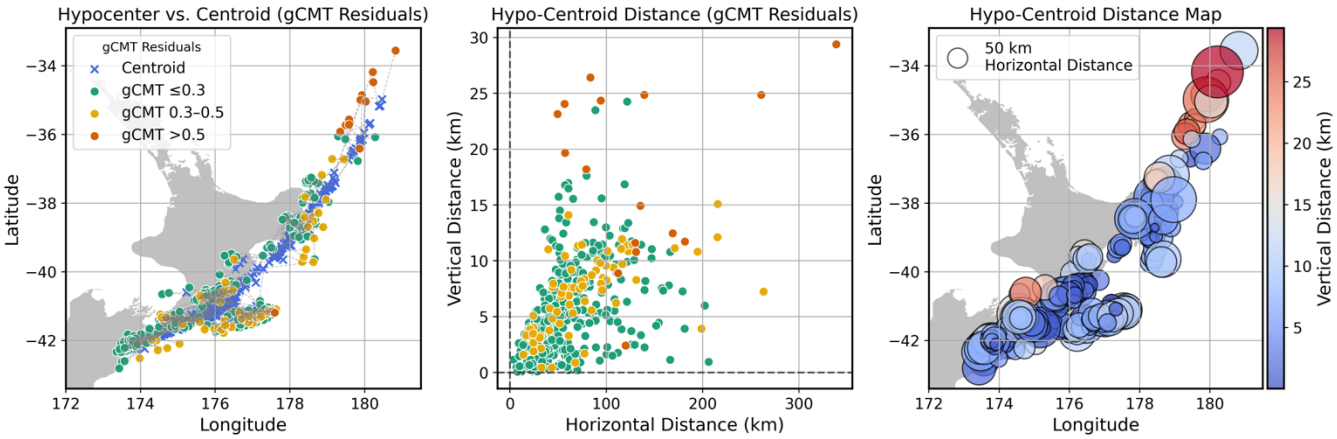

Figure S2. Comparison of hypocenter and centroid locations with magnitude residual (Final – Target) categories for geodetic centroid moment tensor (gCMT) solutions. The left panel shows hypocenter locations (circles) and centroid locations (blue crosses) for gCMT residuals. Hypocenter locations are color-coded by error magnitude: green for low errors (≤0.3), yellow for moderate errors (0.3–0.5), and red for large errors (>0.5), corresponding to varying residual magnitudes. The middle panel presents hypocenter vs. centroid locations for gCMT residuals, following the same residual categorization. The right panel displays a hypocenter map, where marker size and color represent the horizontal and vertical distances, respectively, between the hypocenter and centroid.

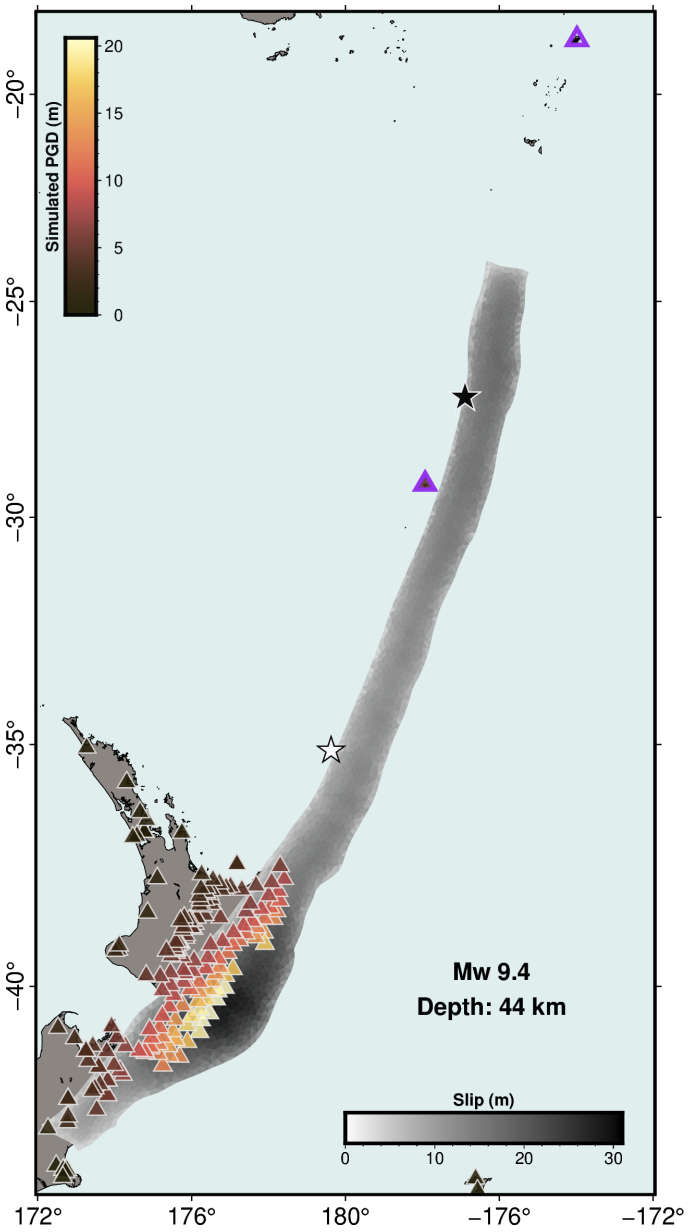

Figure S3. An extraordinary case of a full-rupture **M**9.4 event in the Kermadec-Tonga subduction system, where G-FAST is unable to produce a solution because the stations are too far from the hypocenter to compute a reliable estimate. The map shows observed peak ground displacement (PGD) values at each station (color-filled triangles) within 1000 km, based on the distance from the station to the entire rupture plane (R_p), shown in warm colormap. The grayscale colormap represents the amount of rupture slip for reference. Triangles with thick purple borders indicate stations within 1000 km based on the distance from the station to the hypocenter (R_{hypo}). The black star shows the hypocenter, while the white star represents the centroid location. Labels indicate the magnitude and depth of the event.

References

Crowell, B. W., Schmidt, D. A., Bodin, P., Vidale, J. E., Gomberg, J., Hartog, J. R., Kress, V. C., Melbourne, T. I., Santillan, M., Minson, S. E., & Jamison, D. G. (2016). Demonstration of the Cascadia G-FAST geodetic earthquake early warning system for the Nisqually, Washington, earthquake. *Seismological Research Letters, 87*(4), 930–943. https://doi.org/10.1785/0220150255

Crowell, B. W., Schmidt, D. A., Bodin, P., Vidale, J. E., Baker, B., Barrientos, S., & Geng, J. (2018). G-FAST earthquake early warning potential for great earthquakes in Chile. *Seismological Research Letters, 89*(2A), 542–556. https://doi.org/10.1785/0220170180

Hughes, L., Lane, E. M., Power, W., Savage, M. K., Arnold, R., Howell, A., Liao, Y.-W. M., Williams, C., Shaw, B., Fry, B., & Nicol, A. (2025). Effects of subduction interface locking distributions on tsunami hazard: A case study on the Hikurangi/Tonga-Kermadec subduction zones. *Geophysical Journal International, 240*(2), 1147–1167. https://doi.org/10.1093/gji/ggae441

Goldberg, D. E., Melgar, D., Hayes, G. P., Crowell, B. W., & Sahakian, V. J. (2021). A ground-motion model for GNSS peak ground displacement. *Bulletin of the Seismological Society of America, 111*(5), 2393–2407. https://doi.org/10.1785/0120210042

Richards-Dinger, K., & Dieterich, J. H. (2012). RSQSim earthquake simulator. *Seismological Research Letters, 83*(6), 983–990. https://doi.org/10.1785/0220120105